When Relation Networks meet GANs: Relation GANs with Triplet Loss

Runmin Wu
Dalian University of Technology
josephinerabbit@mail.dlut.edu.cn

Kuyao Zhang
Dalian University of Technology
zhangkunyao@mail.dlut.edu.cn

Lijun Wang
Dalian University of Technology
xingkong19890806@gmail.com

Yue Wang
Dalian University of Technology
ellabear@mail.dlut.edu.cn

Huchuan Lu
Dalian University of Technology
lhchuan@dlut.edu.cn

Yizhou Yu
Deepwise
yizhouy@acm.org

Abstract

Though recent research has achieved remarkable progress in generating realistic images with generative adversarial networks (GANs), the lack of training stability is still a lingering concern of most GANs, especially on high-resolution inputs and complex datasets. Since the randomly generated distribution can hardly overlap with the real distribution, training GANs often suffers from the gradient vanishing problem. A number of approaches have been proposed to address this issue by constraining the discriminator's capabilities using empirical techniques, like weight clipping, gradient penalty, spectral normalization etc. In this paper, we provide a more principled approach as an alternative solution to this issue. Instead of training the discriminator to distinguish real and fake input samples, we investigate the relationship between paired samples by training the discriminator to separate paired samples from the same distribution and those from different distributions. To this end, we explore a relation network architecture for the discriminator and design a triplet loss which performs better generalization and stability. Extensive experiments on benchmark datasets show that the proposed relation discriminator and new loss can provide significant improvement on variable vision tasks including unconditional and conditional image generation and image translation.

1. Introduction

Since first proposed in [9], generative adversarial networks (GANs) have witnessed a rapid development and found numerous applications in many computer vision tasks, such as image generation [9, 14, 44], person re-identification [2], image super-resolution [1] etc. It also has been extended to natural language processing [38], video sequence synthesis [7], and speech synthesis [31] recently.

Though tremendous success has been achieved in many fields, training GANs is still a very tricky process and suffers from many issues, including the instability between the generator and the discriminator as well as the extremely subtle sensitivity to network architecture and hyper-parameters. It has been proved that most of these issues are due to the fact that the support of both target distribution and generated distribution are often of low dimension regarding to the base space, and therefore misaligned at most of the time, causing discriminator to collapse to a function that hardly provides gradients to the generator.

To remedy this issue, recent works proposed to leverage the Integral Probability Metric (IPM), such as Gradient Penalty [10] and Spectral Normalization [29]. In IPM-based GANs, the discriminator is constrained to a specific class of function so that it does not grow too quickly and thus alleviates vanishing gradients.

However, the existing IPM methods also have their limits. For instance, the hyperparameter tuning of gradient penalty is mostly empirical, while the spectral normalization imposes constrains on every conv-layers which hinders the learning capacity of discriminators.

In [14], the authors argue that non-IPM-based GANs are missing a relativistic discriminator, which IPM-based GANs already possess. The relativistic discriminator is necessary to make the training process analogous to divergence minimization and produce sensible predictions based on the prior knowledge that half of the samples in the mini-batch are fake. Although they have shown the power of relativistic discriminator, the potential of comparing the relation between real and fake distribution still remains to be explored.

In this paper, we explicitly study the effect of relation comparison in GANs by training the discriminator to determine whether the input paired samples are drawn from the same distribution (either real or fake). A relation network is present, acting as the discriminator. A new triplet loss is also designed for training the GANs. In this way, the before-mentioned problem of the disjointed support could be alleviated by projecting and merging the low dimension data distribution into a high dimension feature space. Mathematically, we prove our new triplet loss is a divergence and could achieve the Nash equilibrium leading to convergence of the generated data distribution to the real distribution. In addition, we analyze the oscillatory behavior that GANs exhibit for the Dirac-GAN and we demonstrate the proposed Relation GAN is locally convergent even with no regularized methods.

Extensive experiments are conducted on conditional and unconditional image generation and image translation tasks. The promising performance demonstrates the proposed relation gan has great potential in various applications of GANs.

In summary, the contributions of this paper are two folds.

- We propose a new training strategy for GANs to better leverage the relation between samples. Instead of separating real samples from generated ones, the discriminator is trained to determine whether a paired samples are from the same distribution.
- We propose a relation network architecture as the discriminator and a triplet loss for training GANs. We show both theoretically and empirically that the relation network together with the triplet loss give rise to generated density which can exactly match that of real data.

Extensive experiments on 2D grid [28], Stacked MNIST [18], CelebA [22], LSUN [42], CelebA-HQ [23] data sets confirm our proposed method performs favourably against state-of-the-arts such as relativistic GAN [14], WGAN-GP [10], Least Squares GAN (LSGAN) [25] and vanilla GAN [9].

2. Related Work

The vanilla GAN [9] minimizes the JS divergence of two distributions, leading to the gradient vanishing problem when the two distributions are disjoint. Recent works try to address this issue by designing new objective functions [25, 32, 37, 3] or more sophisticated network architectures [15, 45, 6, 33]. Others investigate the regularization and/or normalization to constrain the ability of discriminator [29, 10, 17]. Recently, a new method [14] is proposed to explore a relativistic discriminator. In the following, we will review recent works using different objective functions and a special case–relativistic GANs, which are closely related to our approaches.

2.1. Different Objective Functions in GANs

Generally, there are two kind of loss functions in GANs: the minimax GAN and the non-saturating (NS) GAN. In the former the discriminator minimizes the negative log-likelihood for the binary classification task. In the latter the generator maximizes the probability of generated samples being real. The non-saturating loss as it is known to outperform the minimax variant empirically. Among them, loss sensitive GAN [32] tries to solve the problem of gradient vanishing by focusing on training samples with low authenticity. WGAN [3] proposes the Wasserstein distance to replace the JS divergence, which can measure their distance even though the two distributions are disjoint. In addition, [3] also proposes to add noise to both real and generated samples to further alleviate the impact of disjoint distributions. [10] improves WGAN by replacing the weight clipping constraints with a gradient penalty, which enforces the Lipschitz constraint on the discriminator by punishing the norm of the gradient. DRAGAN [17] combines the two parts of WGAN and LSGAN, and only improves the loss function to a certain extent. The stability of loss training is controlled by constantly updating the coefficient of the latter term.

2.2. Relativistic GANs

Instead of training discriminators to predict the absolute probabilities of the input samples being real, the relativistic GAN [14] proposes to use a relativistic discriminator, which estimates the probability of the given real sample being more realistic than a randomly sampled fake sample. Although bears a similar spirit, our method differs from [14] in that we adopt a relation network as the discriminator to estimate the relation score of a paired input. In comparison, the discriminator in [14] treats input samples separately and relies on a ranking loss (*e.g.*, hinge loss) to explore their relation. The idea of merging the features and comparing the relation between samples from two distribution has not been explored in the literature of GANs. In addition, our method proposes a new triplet loss to leverage the power of paired relation comparison, allowing more stability and better diversity for GANs without applying any IPM methods.

3. The Relation GAN Framework

3.1. Relation Net Architecture

In traditional GANs, a discriminator is trained to distinguish real samples from fake ones and a generator is trained to confuse the discriminator by generating realistic samples. Consider a real data distribution P_{data}, and the data distri-

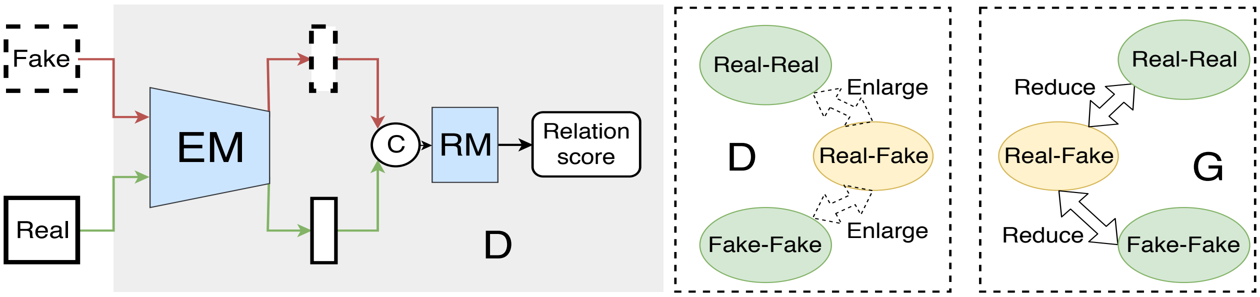

Figure 1. Illustration of our Relation GAN, the "C" denotes contact operation. Our discriminator consists of two modules, an embedding module (EM) and a relation module (RM). The relation discriminator is expected to enlarge the difference of relation score between asymmetric pairs and symmetric pairs while the generator is expected to reduce the difference.

bution P_{G^*} produced by the generator G. Rather than training the discriminator on real and fake data independently, we propose to train a discriminator which predicts a relation score $D(x^1, x^2)$ for a paired input, indicating whether the paired samples are from the same distribution (either P_{data} or P_{G^*}).

Inspired by the success of relation net architecture in other computer vision areas [39], our discriminator consists of two modules, including an embedding module and a relation module as shown in Figure 1. For a pair of input samples, the embedding module firstly maps each sample into a high dimensional feature space. Their corresponding features are then merged and fed into the relation module to produce the relation score for the input pair. For ease of description, we name paired inputs containing both real and fake samples as **asymmetric pairs**, and those containing samples from the same distribution (either real or fake) as **symmetric pairs**. The training process is then formulated as a min-max game (See Section 3.2), where the discriminator aims to maximize the relation scores of asymmetric sample pairs and minimize those of symmetric ones. Meanwhile, the generator is trained to confuse the discriminator by minimizing the relation scores of asymmetric sample pairs containing real and generated samples.

3.2. The Min-Max Game

The min-max game in training GANs is conducted by optimizing the losses of D and G iteratively. In the no-IPM GANs, the generalized losses of D and G can be presented as follows:

$$L_D = \mathbb{E}_{x \sim \mathbb{P}_{data}, y \sim \mathbb{P}_{G^*}}[\tilde{f}(D(x), D(y))] \tag{1}$$

and

$$L_G = \mathbb{E}_{x \sim \mathbb{P}_{data}, y \sim \mathbb{P}_{G^*}}[\tilde{g}(D(x), D(y))] \tag{2}$$

where $\tilde{f}$ and $\tilde{g}$ are scalar-to-scalar functions, $\mathbb{P}_{data}$ is the distribution of real data, and P_{G^*} denotes the generated data distribution.

Let $\tilde{f}(x, y) = -log(x) - log(1-x)$, and $\tilde{g}(x, y) = -log(y)$. Eq (1) and (2) will become the loss functions of the standard GAN [9]. y from P_{G^*} and x from P_{data}.

In our Relation GAN, the formulation of the losses functions of D and G are as follows:

$$L_D = \mathbb{E}_{x_r \sim \mathbb{P}_{data}, y_f \sim \mathbb{P}_{G^*}}[\tilde{f}(D(x_r^1, x_r^2), D(y_f^1, y_f^2), D(x_r^1, y_f^1))] \tag{3}$$

and

$$L_G = \mathbb{E}_{x_r \sim \mathbb{P}_{data}, y_f \sim \mathbb{P}_{G^*}}[\tilde{g}(D(x_r^1, x_r^2), D(y_f^1, y_f^2), D(x_r^1, y_f^1))] \tag{4}$$

where $\tilde{f}$ and $\tilde{g}$ are also scalar to scalar function.

The goal of relation discriminator is to learn a loss function D_θ parameterized by θ which separates symmetric and asymmetric sample pairs by a desired margin. Then the generator can be trained to minimize this margin by generating realistic samples.

Inspired by the success of triplet loss [8], we formulate the similar loss function in our Relation GAN as follows:

$$\begin{aligned} L_D =& \mathbb{E}_{x_r \sim \mathbb{P}_{data}, y_f \sim \mathbb{P}_{G^*}}[(D(x_r^1, x_r^2) - D(x_r^1, y_f^1) + \Delta(x_r^2, y_f^1)]_+ \\ &+ \mathbb{E}_{x_r \sim \mathbb{P}_{data}, y_f \sim \mathbb{P}_{G^*}}[(D(y_f^1, y_f^2) - D(x_r^1, y_f^1) + \Delta(y_f^2, x_r^1)]_+ \end{aligned} \tag{5}$$

and

$$\begin{aligned} L_G =& \mathbb{E}_{x_r \sim \mathbb{P}_{data}, y_f \sim \mathbb{P}_{G^*}}[D(x_r^1, y_f^1)] - \mathbb{E}_{x_r \sim \mathbb{P}_{data}}[D(x_r^1, x_r^2)] \\ &+ \mathbb{E}_{x_r \sim \mathbb{P}_{data}, y_f \sim \mathbb{P}_{G^*}}[D(x_r^1, y_f^1)] - \mathbb{E}_{y_f \sim \mathbb{P}_{G^*}}[D(y_f^1, y_f^2)] \\ =& 2\mathbb{E}_{x_r \sim \mathbb{P}_{data}, y_f \sim \mathbb{P}_{G^*}}[D(x_r^1, y_f^1)] - \mathbb{E}_{y_f \sim \mathbb{P}_{G^*}}[D(y_f^1, y_f^2)] \end{aligned}$$

where x_r^1 and x_r^2 are samples from the real data distribution, y_f^1 is sample from the generated data distribution and y_f^2 is sample from the data generated by the generator in the last step of optimization. We use a distance metric to replace the constant 'margin' in the original triplet loss. This variable constraining leads to a smaller difference of relation scores when the distance between the two compared samples are smaller, which is more flexible than the original fixed margin. Our experiments also shows the superiority of our new triplet loss with Δ margin.

3.3. A Variant Loss

Since the training batch size is limited, the sampled distribution of each batch may deviates from the real data distribution. For an input batch of m paired samples, the loss function in (6) can be written as follows:

$$\begin{aligned} L_D =& \frac{1}{m}\sum\nolimits_{i=1}^{m}[(D(x_r^{1i}, x_r^{2i}) - D(x_r^{1i}, y_f^{1i}) + \Delta(x_r^{2i} y_f^{1i})]_+ \\ &+ \frac{1}{m}\sum\nolimits_{i=1}^{m}[(D(y_f^{1i}, y_f^{2i}) - D(x_r^{1i}, y_f^{1i}) + \Delta(y_f^{2i}, x_r^{1i})]_+ \end{aligned} \tag{6}$$

where $x_r \sim \mathbb{P}_{data}, y_f \sim \mathbb{P}_{G^*}$. Our triplet loss is designed to reduce the relation scores of symmetric sample pairs and increase those of asymmetric ones.

However, when the real sample distribution is fairly uniform with small variance, the original loss is rigorous and prone to be disturbed by outliers in one batch. For these cases, we design a variant of our new triplet loss as follows:

$$\begin{aligned} L_D =& [(\frac{1}{m}\sum\nolimits_{i=1}^{m} D(x_r^{1i}, x_r^{2i}) - \frac{1}{m}\sum\nolimits_{i=1}^{m} D(x_r^{1i}, y_f^{1i}) \\ &+ \frac{1}{m}\sum\nolimits_{i=1}^{m} \Delta(x_r^{2i} y_f^{1i})]_+ \\ &+ [\frac{1}{m}\sum\nolimits_{i=1}^{m}(D(y_f^{1i}, y_f^{2i}) - \frac{1}{m}\sum\nolimits_{i=1}^{m} D(x_r^{1i}, y_f^{1i}) \\ &+ \frac{1}{m}\sum\nolimits_{i=1}^{m} \Delta(y_f^{2i}, x_r^{1i})]_+ \end{aligned} \tag{7}$$

where i represents the index of samples in a batch. The variant loss is more relaxed and not easily disturbed by the extreme samples in the same batch. It performs better on evenly distributed data sets.

Thus, we suggest to employ the variant triplet loss on uniform distribution data, e.g., datasets with only single class data. Our experiments results on the dataset of single class such as, CelebA and LSUN confirm it.

4. Theory Proof and Analysis

As discussed in the introduction, the optimal discriminator of most GANs is a divergence. In this section, we firstly prove that the proposed discriminator based on the relation net also has such property, and then show the distributional consistency under our Lipschitz continuous assumption.

4.1. A New Divergence

A divergence is a function $\mathcal{M}$ of two variables p, q satisfies the following definition:

Definition 1 If $\mathcal{M}$ is function of two variables p, q satisfies the following properties:

1. $\mathcal{M}[p, q] \geq 0$
2. $p = q \Leftrightarrow \mathcal{M}[p, q] = 0$

Then $\mathcal{M}$ is a divergence between p and q.

Assumption 1 In the training process, when G not reach the optimal G^*, y_f^1 ought to be more realistic than y_f^2, and D ought to give bigger relation score to the paired input (y_f^1, y_f^2) than (x_r^1, x_r^2). y_f^1 ought to be more realistic than y_f^2 also means, $\Delta(y_f^2, x_r)$ is bigger than $\Delta(y_r^1, x_r)$

Under this assumption, we show the loss function of our relation discriminator L_D is also a divergence in **Supplementary 1**.

4.2. Distributional Consistency

We use θ to denote the parameterized function discriminator and ϕ to denote the parameterized function of generator. Based on [32], we use the definition of Lipschitz assumption of data density as follows:

Definition 2 For any two samples x and z, the loss function $F(x)$ is Lipschitz continuous with respect to a distance metric Δ if

$$|F(x) - F(z)| \leq \kappa\Delta(x, z)$$

with a bounded Lipschitz constant k, *i.e.*, $k < +\infty$

Assumption 2 The data density P_{data} is supported in a compact set $\mathcal{D}$, and it is Lipschitz continuous wrt Δ with a bounded constant $k < +\infty$ which is satisfied with Definition 2. Then we show the existence of Nash equilibrium such that both the function D_{θ^*} and the density P_{G^*} of generated samples are Lipschitz. Same as the [32], we have both $L_D(\theta, \phi)$ and $L_G(\theta, \phi)$ are convex in D_{θ^*} and in P_{G^*}. Then, according to the Sions theorem [36], with D_{θ^*} and P_{G^*} being optimized, there exists a Nash equilibrium (θ^*, ϕ^*) We also have the following lemma.

Under Assumption 2, there exists a Nash equilibrium (θ^*, ϕ^*) such that both D_{θ^*} and P_{G^*} are Lipschitz.Then we could prove that when reaching the Nash equilibrium, the density distribution $\mathbb{P}_{G^*}$ of the samples generated by G will converge to the real data distribution $\mathbb{P}_{data}$, which is the lemma 1 as follows:

Lemma 1 Under Assumption 2, for a Nash equilibrium (θ^*, ϕ^*) in Lemma 1, we have

$\int_{\mathbf{x}} |P_{\text{data}}(x) - P_{G^*}(x)| dx \leq 0$

Thus, $P_{G^*}(x)$ converges to $P_{data}(x)$. The proof of this lemma is given in the **Supplementary 2**.

4.3. The Convergence

In the literature, GANs are often treated as dynamic systems to study their training convergence [26], [27], [30], [12]. This idea can be dated back to the Dirac GAN [26], which describes a simple yet prototypical counterexample for understanding whether the GAN training is locally nor globally convergent. To further analyze the convergence rate of training the proposed Relation GAN, we also adopt the Dirac GAN theory. However, [26] only discusses the situation where the data

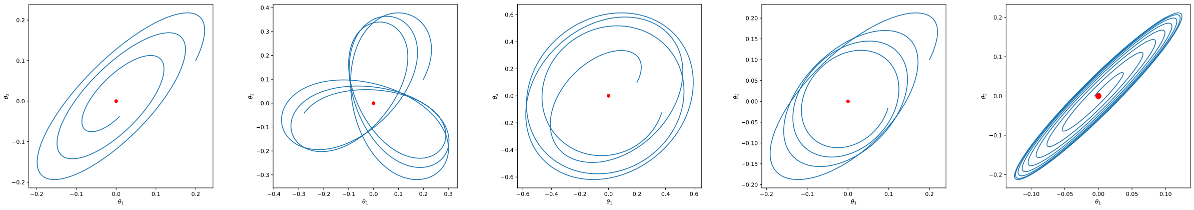

(a) Vanilla GAN (b) WGAN (c) WGAN-GP (d) GAN-QP (e) Relation GAN

Figure 2. The numerical solution on Dirac GANs

distributions are 1-D. We extend this theory into the 2-D case to gain better understanding.

Definition 3 The Dirac-GAN consists of a (univariate) generator distribution $p_\theta = \delta_\theta$ and a linear discriminator $D(x) = \phi \cdot x$, where θ denotes the parameter of the generator, x is a 2-D vector, and ϕ represents the parameter of the discriminator. The real data distribution p_{data} is a Dirac-distribution concentrated at $(0, 0)$.

Suppose the real sample point is a vector $(0, 0)$, and the fake sample is being reorganized, which also represents a parameter of the generator. The discriminator uses the simplest linear model, *i.e.*, $D(x) = x$, which also represents the parameters of the discriminator. Dirac GAN takes into account that in such a minimalist model, whether a false sample eventually converges to a true sample, in other words, whether a finally converges to $(0, 0)$. Specifically, in Relation GAN, our Dirac Discriminator could be simplified as: $D(x^1, x^2) = \theta_r(\theta_e \cdot x^1 + \theta_e \cdot x^2)$, where θ_r and θ_e denotes the parameter of the embedding module and relation module respectively.

Based on the dynamic analysis for GANs in **Supplementary 3**, we have the numerical solution of the GANs' dynamic equations with a initial point $(0.2, 0.1)$ as the fig 2 shows. In [26], the author find that most unregulared GANs are not locally convergent. In our 2-D Dirac GANs, the numerical solutions of the WGAN [3], WGAN-GP [10], GAN-QP [37], vanilla GAN [9] also perform oscillating near the real sample or hard to converge to the real sample point, while our Relation GAN success to converge. It indicates that our GAN has a good local convergence.

5. Experiments

We first evaluate the proposed Relation GAN on the 2D synthetic dataset and the Stacked MNIST dataset to demonstrate the diversity of generated data and the stability of generator. We then perform the image generation tasks with our method to show its superiority in synthesizing natural images. Finally, ablation study is conducted to verify the effects of the feature merging mechanism in relation nets and the proposed triplet loss.

5.1. The Diversity of Generated Data

2D Datasets We compare the effect of our relation discriminator on the 2D 8-Gaussian distribution, 2D 25-Gaussian distribution and 2D swissroll distribution. The experimental settings follow [41]. The results generated by our method and four popular methods under the same setting are shown in Figure 3. Compared with the other methods, ours can better fit these 2D distributions.

Stacked MNIST For Stacked MNIST [18] experiments, we use the setting and code of [41]. Each of the three channels in each sample is classified by a pre-trained MNIST classifier, and the resulting three digits determine which of the 1000 modes the sample belongs to. We measure the number of modes captured with the pre-trained classifier. We choose Adam [16] optimizer for all experiments. Our results are shown in Table 1. We find that our Relation GAN could achieve best mode coverage, reaching all 1,000 modes.

Table 1. Stacked MNIST

Loss	Modes
LSGAN	985±10
WGANGP	643±7
Vanilla GAN	923±18
Relativastic GAN	828±58
Ours	1000±0

5.2. Unconditional Image Generation

Datasets We provide comparison on four datasets, namely CIFAR-10 [5], CelebA [22], LSUN-BEDROOM [42] and CelebA-HQ [23]. The LSUN-BEDROOM dataset [42] contains 3M images which are randomly partitioned into a test set of around 30k images and a training set containing the rest. We use $128 \times 128 \times 3$ version of CelebA-HQ with 30k images. We only compare our method with Relativistic GAN and WGANGP on CelebA-HQ due to limited computation resources.

Settings For CIFAR-10, we use the Resnet [11] architecture proposed in [41](with spectral normalization layers removed). For CelebA, LSUN and CelebA-HQ, we used a DCGAN architecture as in [29]. We apply

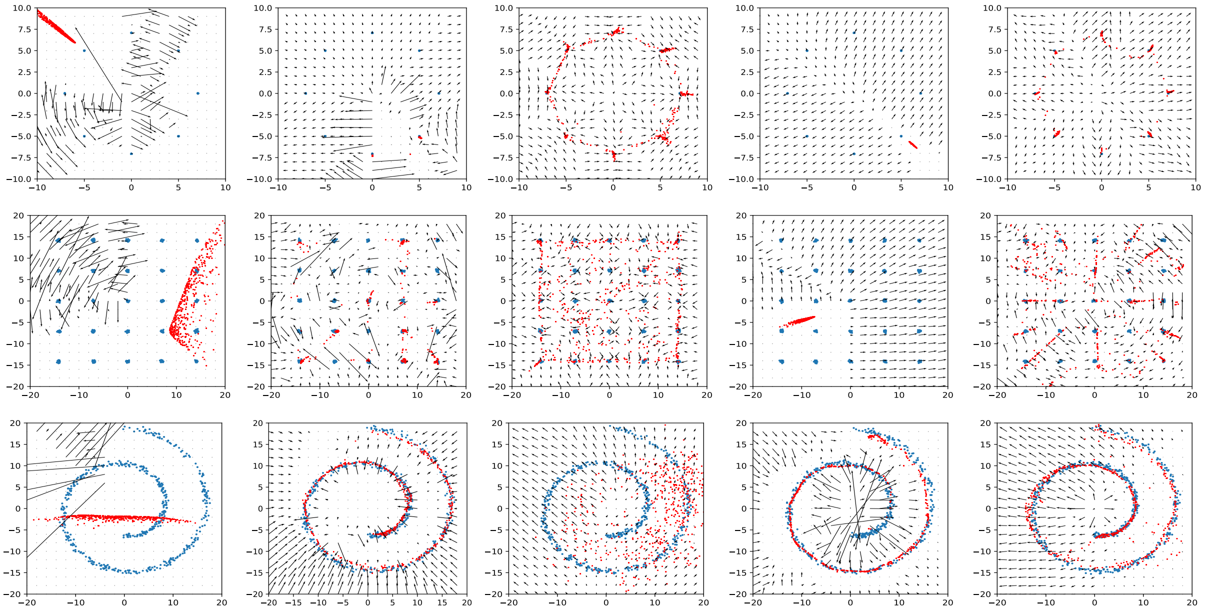

(a) Vanilla GAN (b) LSGAN (c) WGAN-GP (d)Relativistic GAN (e) Relation GAN

Figure 3. Comparison on 2D datasets.

Adam optimizer on all experiments as Table 2 shows. We used 1 discriminator updates per generator update. The batch size used was 64. Other details of our experiments settings are provided in **Supplementary**.

Table 2. Experiments Settings

Dataset	lr_g	lr_d	β_1	β_2	Iterations
CIFAR-10	0.0002	0.0001	0.9	0.999	600k
CelebA	0.0002	0.0001	0.9	0.999	400k
LSUN	0.0001	0.0001	0	0.9	400k
CelebA-HQ	0.0001	0.0001	0	0.9	250k

Evaluation To compare the sample quality of different models, we consider three different scores: IS [35], FID [12] and KID [4] which are based on the pre-trained Inception network [40] on ImageNet [34].

Results and Analysis Some random generated samples on 3 data sets are shown in Figure **??**. More generated images and evaluation scores are provided in **Supplementary 6**. From Table 3 we could find RelatioGAN* is also highly competitive on single class data sets *i.e.* CelebA, LSUN, while RelationGAN achieves the best performance on CIFAR-10. As we discussed in Sec.3.3, the variant loss of $Ours^*$ is more relaxed and suitable for evenly distributed data sets while the loss of $Ours$ in eq. (6) is more strict and performs better on multi-class or harder data sets (also performs best on Stacked MNIST).

5.3. Conditional Image Generation

We compare the MSGAN [24] which is one of the best conditional gan model on conditonal CIFAR-10 datasets. The experiment is applied by simply replace the MS-loss in [24] with the relation loss. Table 4 represents the results of FID.

5.4. Image Translation

In addition to image generation task, GANs also gains promising progress in image translation task. It has been shown a great success in ranges of image translation tasks, including style transfer, image enhance, image super resolution and image segmentation. We conduct three relative experiments on image style transfer and image super resolution, respectively.

Image Style Transfer For image style transfer task, we adopt the CycleGAN as our baseline model to translate Monets painting into photograph. Fig xx shows the visual comparison with results of our methods and xxx. FID score is applied to evaluate the quality of generated images. Table 5 shows the comparison of fid scores of generated images. The lower fid represents smaller perceptual difference between target domain images and generated images. We find the both relation loss* and relation loss performs better than the oigianl adversarial loss in cycle-gan and the reltion loss* performs best.

Image Super Resolution For Image Super Resolution task, we employ SRGAN [19] with the relasitvistc loss which is the latest proposed loss for gans as our baseline. We denote our baseline as SRGAN*. The train and val datasets are sampled from VOC2012. Train dataset has 16700 images and Val dataset has 425 images. We compare the psrn and ssim on three popular SR datasets: Set5 [43],

Table 3. The Comparisons of FID, KID Score and IS. RelationGAN represents Relation GAN with objective function in equation (6) and RelationGAN* represents Relation GAN with objective function in equation (7). The best two scores are shown in red and green, respectively.

	CIFAR-10			CelebA		
	FID	KID	IS	FID	KID	IS
Vanilla GAN	26.46±0.12	1.88±0.061	6.73±0.081	34.43±0.15	3.01±0.044	2.68±0.020
LS-GAN	14.9±0.061	1.31±0.056	7.74±0.12	19.63±0.11	1.84±0.045	2.5±0.021
WGAN-GP	63.56±0.14	8.01±0.068	3.56±0.038	66.06±0.27	9.06±0.081	2.60±0.029
Relativistic	23.96±0.15	1.88±0.061	0.061±0.081	26.71±0.10	2.08±0.050	3.02±0.024
RelationGAN	13.52±0.060	1.26±0.052	7.74±0.18	25.37±0.14	2.07±0.044	2.65±0.029
RelationGAN*	47.96±0.30	8.88±0.072	3.32±0.026	11.99±0.064	1.10±0.038	3.17±0.036

	LSUN			CelebA-HQ		
	FID	KID	IS	FID	KID	IS
Vanilla GAN	38.17-±0.28	6.61±0.076	4.57±0.010	–	–	–
LS-GAN	150.61±0.33	21.75±0.11	3.57±0.043	–	–	–
WGAN-GP	14.93±0.16	1.45±0.042	3.77±0.098	68.5±0.19	7.71±0.065	2.31 ±0.017
Relativistic	40.84±0.23	2.97±0.045	4.08±0.049	32.24±0.21	2.27 ±0.056	1.96±0.038
RelationGAN	70.24±0.37	5.89±0.078	4.4±0.056	27.87±0.17	2.21±0.047	2.13±0.0052
RelationGAN*	12.59±0.11	1.37±0.038	3.70±0.081	26.17±0.12	2.62±0.043	2.15±0.030

Table 4. The comparison of FID scores on the CIFAR-10 dataset.

	MSGAN	RelationGAN
FID	28.73	**24.88**

Table 5. The Comparison of FID Scores on Style Transfer Results. The M→P represents painting to photo, the P→M represents photo to painting. RelationGAN and RelationGAN* represents loss equation 6 and equation 7, respectively.

	FID(M→P)	FID(P→M)
CycleGAN	34.00	2.48
RelationGAN	**33.60**	2.26
RelationGAN*	33.71	**2.21**

Table 6. Comparison of SRGAN* and RelationGAN on benchmark data. Highest measures (PSNR (dB), SSIM) in bold. (4 upscaling)

	Set5		Set14		Urban100	
	psnr	ssim	psnr	ssim	psnr	ssim
SRGAN*	28.40	0.82	25.37	0.73	23.36	0.71
RelationGAN	**28.59**	**0.83**	**25.52**	**0.73**	**23.47**	**0.72**

Set14 [20] and Urban100 [13]. The Figure **??** shows some visual results.

Table 6 lists the psnr and ssim of different approaches on five datasets. We can observe that the fid scores of the proposed algorithm perform better than the original method on photo→painting datasets.

5.5. Ablation Study

We conduct the ablation study on image generation datasets. We first compare our triplet loss with the siamese loss [8], whose results are shown in Table 7. The formulation of siamese loss function is shown in **Supplementary 4**. Second, we take a closer look on the impact of our embedding module and relation module. The "$n + m$" in the Table 8 represents different architectures of discriminator, where the embedding module contains n res-block and the relation module contains m res-block. The "(0+3)" represents the samples are contacted together after first conv-layer and then put into the relation module (RM) which contains 3 res-block. The "no EM" represents the samples in which the paired input are packed in the beginning of the discriminator as [21]. All experiments are conducted on CIFAR-10.

Table 7. Ablation Losses

	CIFAR-10	CelebA
Triplet	13.42	11.9
Siamese	–	107.3

Table 8. Results of Different Architectures

	FID(CIFAR-10)
no EM	38.9
$0 + 3$	37.37
$1 + 2$	28.89
$2 + 1$	28.80
$3 + 0$	13.52

Results and Analysis From Table 7, we could find the results of the proposed triplet loss is much better than Siamese loss. The "-" represents model collapse in training process. The results in Table 8 shows the bigger size of EM could enhance the performance which also demonstrates the effectiveness of our embedding strategy.

6. Conclusion

In this paper we propose the Relation GANs. A relation network architecture is designed and used as the discriminator, which is trained to determine whether a paired input samples are from the same distribution or not. The generator is jointly trained with the discriminator to confuse its decision using a triplet loss.

Mathematically, we prove that the optimal discriminator based on the relation network is a divergence, indicating the distance of generated data distribution and the real data distribution becomes progressively smaller during the training process. We also prove the generated data distribution will converge to the real data distribution when getting to the Nash equilibrium. In addition, we analysis our method and several other GANs in dynamic system. We demonstrate our GAN has excellent convergence by analyzing the dynamic system of the Dirac GANs.

The results of experiments on simple 2D distribution data and Stacked MNIST verify the effectiveness of Relation GAN, especially in addressing the mode collapse problem. Our Relation GAN not only achieves state-of-the-art performance on unconditional and conditional image generation task with the basic architecture and training settings, but also achieves promising results in image translation tasks compared with other gan losses.

References

[1] *Photo-Realistic Single Image Super-Resolution Using a Generative Adversarial Network*, 2017. 1

[2] *Advances in Neural Information Processing Systems 31: Annual Conference on Neural Information Processing Systems 2018, NeurIPS 2018, 3-8 December 2018, Montréal, Canada*, 2018. 1

[3] Martín Arjovsky, Soumith Chintala, and Léon Bottou. Wasserstein generative adversarial networks. In *Proceedings of the 34th International Conference on Machine Learning, ICML 2017, Sydney, NSW, Australia, 6-11 August 2017*, pages 214–223, 2017. 2, 5

[4] Mikolaj Binkowski, Dougal J. Sutherland, Michael Arbel, and Arthur Gretton. Demystifying MMD gans. In *6th International Conference on Learning Representations, ICLR 2018, Vancouver, BC, Canada, April 30 - May 3, 2018, Conference Track Proceedings*, 2018. 6

[5] Y-Lan Boureau, Francis R. Bach, Yann LeCun, and Jean Ponce. Learning mid-level features for recognition. In *The Twenty-Third IEEE Conference on Computer Vision and Pattern Recognition, CVPR 2010, San Francisco, CA, USA, 13-18 June 2010*, pages 2559–2566, 2010. 5

[6] Andrew Brock, Jeff Donahue, and Karen Simonyan. Large scale GAN training for high fidelity natural image synthesis. *CoRR*, abs/1809.11096, 2018. 2

[7] Haoye Cai, Chunyan Bai, Yu-Wing Tai, and Chi-Keung Tang. Deep video generation, prediction and completion of human action sequences. In *Computer Vision - ECCV 2018 - 15th European Conference, Munich, Germany, September 8-14, 2018, Proceedings, Part II*, pages 374–390, 2018. 1

[8] Vijay Kumar B. G, Gustavo Carneiro, and Ian D. Reid. Learning local image descriptors with deep siamese and triplet convolutional networks by minimizing global loss functions. In *2016 IEEE Conference on Computer Vision and Pattern Recognition, CVPR 2016, Las Vegas, NV, USA, June 27-30, 2016*, pages 5385–5394, 2016. 3, 7

[9] Ian J. Goodfellow, Jean Pouget-Abadie, Mehdi Mirza, Bing Xu, David Warde-Farley, Sherjil Ozair, Aaron C. Courville, and Yoshua Bengio. Generative adversarial nets. In *Advances in Neural Information Processing Systems 27: Annual Conference on Neural Information Processing Systems 2014, December 8-13 2014, Montreal, Quebec, Canada*, pages 2672–2680, 2014. 1, 2, 3, 5

[10] Isabelle Guyon, Ulrike von Luxburg, Samy Bengio, Hanna M. Wallach, Rob Fergus, S. V. N. Vishwanathan, and Roman Garnett, editors. *Advances in Neural Information Processing Systems 30: Annual Conference on Neural Information Processing Systems 2017, 4-9 December 2017, Long Beach, CA, USA*, 2017. 1, 2, 5

[11] Kaiming He, Xiangyu Zhang, Shaoqing Ren, and Jian Sun. Deep residual learning for image recognition. In *2016 IEEE Conference on Computer Vision and Pattern Recognition, CVPR 2016, Las Vegas, NV, USA, June 27-30, 2016*, pages 770–778, 2016. 5

[12] Martin Heusel, Hubert Ramsauer, Thomas Unterthiner, Bernhard Nessler, and Sepp Hochreiter. Gans trained by a two time-scale update rule converge to a local nash equilibrium. In *Advances in Neural Information Processing Systems 30: Annual Conference on Neural Information Processing Systems 2017, 4-9 December 2017, Long Beach, CA, USA*, pages 6629–6640, 2017. 4, 6

[13] Jia-Bin Huang, Abhishek Singh, and Narendra Ahuja. Single image super-resolution from transformed self-exemplars. In *IEEE Conference on Computer Vision and Pattern Recognition, CVPR 2015, Boston, MA, USA, June 7-12, 2015*, pages 5197–5206, 2015. 7

[14] Alexia Jolicoeur-Martineau. The relativistic discriminator: a key element missing from standard GAN. *CoRR*, abs/1807.00734, 2018. 1, 2

[15] Tero Karras, Timo Aila, Samuli Laine, and Jaakko Lehtinen. Progressive growing of gans for improved quality, stability, and variation. In *6th International Conference on Learning Representations, ICLR 2018, Vancouver, BC, Canada, April 30 - May 3, 2018, Conference Track Proceedings*, 2018. 2

[16] Diederik P. Kingma and Jimmy Ba. Adam: A method for stochastic optimization. *CoRR*, abs/1412.6980, 2014. 5

[17] Naveen Kodali, Jacob D. Abernethy, James Hays, and Zsolt Kira. On convergence and stability of gans. *CoRR*, 2018. 2

[18] Yann LeCun, Bernhard E. Boser, John S. Denker, Donnie Henderson, Richard E. Howard, Wayne E. Hubbard, and Lawrence D. Jackel. Handwritten digit recognition with a back-propagation network. In *Advances in Neural Information Processing Systems 2, [NIPS Conference, Denver, Colorado, USA, November 27-30, 1989]*, pages 396–404, 1989. 2, 5

[19] Christian Ledig, Lucas Theis, Ferenc Huszar, Jose Caballero, Andrew Cunningham, Alejandro Acosta, Andrew P. Aitken, Alykhan Tejani, Johannes Totz, Zehan Wang, and Wenzhe Shi. Photo-realistic single image super-resolution using a generative adversarial network. In *2017 IEEE Conference on Computer Vision and Pattern Recognition, CVPR 2017, Honolulu, HI, USA, July 21-26, 2017*, pages 105–114, 2017. 6

[20] Xin Li and Michael T. Orchard. New edge-directed interpolation. *IEEE Trans. Image Processing*, 10(10):1521–1527, 2001. 7

[21] Zinan Lin, Ashish Khetan, Giulia C. Fanti, and Sewoong Oh. Pacgan: The power of two samples in generative adversarial networks. In *Advances in Neural Information Processing Systems 31: Annual Conference on Neural Information Processing Systems 2018, NeurIPS 2018, 3-8 December 2018, Montréal, Canada.*, pages 1505–1514, 2018. 7

[22] Ziwei Liu, Ping Luo, Xiaogang Wang, and Xiaoou Tang. Deep learning face attributes in the wild. In *2015 IEEE International Conference on Computer Vision, ICCV 2015, Santiago, Chile, December 7-13, 2015*, pages 3730–3738, 2015. 2, 5

[23] Mario Lucic, Karol Kurach, Marcin Michalski, Sylvain Gelly, and Olivier Bousquet. Are gans created equal? a large-scale study. In *Advances in Neural Information Processing Systems 31*, pages 700–709, 2018. 2, 5

[24] Qi Mao, Hsin-Ying Lee, Hung-Yu Tseng, Siwei Ma, and Ming-Hsuan Yang. Mode seeking generative adversarial networks for diverse image synthesis. In *IEEE Conference on Computer Vision and Pattern Recognition, CVPR 2019, Long Beach, CA, USA, June 16-20, 2019*, pages 1429–1437, 2019. 6

[25] Xudong Mao, Qing Li, Haoran Xie, Raymond Y. K. Lau, Zhen Wang, and Stephen Paul Smolley. Least squares generative adversarial networks. In *IEEE International Conference on Computer Vision, ICCV 2017, Venice, Italy, October 22-29, 2017*, pages 2813–2821, 2017. 2

[26] Lars M. Mescheder, Andreas Geiger, and Sebastian Nowozin. Which training methods for gans do actually converge? In *Proceedings of the 35th International Conference on Machine Learning, ICML 2018, Stockholmsmässan, Stockholm, Sweden, July 10-15, 2018*, pages 3478–3487, 2018. 4, 5

[27] Lars M. Mescheder, Sebastian Nowozin, and Andreas Geiger. The numerics of gans. In *Advances in Neural Information Processing Systems 30: Annual Conference on Neural Information Processing Systems 2017, 4-9 December 2017, Long Beach, CA, USA*, pages 1823–1833, 2017. 4

[28] Luke Metz, Ben Poole, David Pfau, and Jascha Sohl-Dickstein. Unrolled generative adversarial networks. In *5th International Conference on Learning Representations, ICLR 2017, Toulon, France, April 24-26, 2017, Conference Track Proceedings*, 2017. 2

[29] Takeru Miyato, Toshiki Kataoka, Masanori Koyama, and Yuichi Yoshida. Spectral normalization for generative adversarial networks. *CoRR*, abs/1802.05957, 2018. 1, 2, 5

[30] Vaishnavh Nagarajan and J. Zico Kolter. Gradient descent GAN optimization is locally stable. In *Advances in Neural Information Processing Systems 30: Annual Conference on Neural Information Processing Systems 2017, 4-9 December 2017, Long Beach, CA, USA*, pages 5591–5600, 2017. 4

[31] Santiago Pascual, Antonio Bonafonte, and Joan Serrà. SEGAN: speech enhancement generative adversarial network. *CoRR*, abs/1703.09452, 2017. 1

[32] Guo-Jun Qi. Loss-sensitive generative adversarial networks on lipschitz densities. *CoRR*, abs/1701.06264, 2017. 2, 4

[33] Alec Radford, Luke Metz, and Soumith Chintala. Unsupervised representation learning with deep convolutional generative adversarial networks. In *4th International Conference on Learning Representations, ICLR 2016, San Juan, Puerto Rico, May 2-4, 2016, Conference Track Proceedings*, 2016. 2

[34] Olga Russakovsky, Jia Deng, Hao Su, Jonathan Krause, Sanjeev Satheesh, Sean Ma, Zhiheng Huang, Andrej Karpathy, Aditya Khosla, Michael Bernstein, Alexander C. Berg, and Li Fei-Fei. ImageNet Large Scale Visual Recognition Challenge. *International Journal of Computer Vision (IJCV)*, 115(3):211–252, 2015. 6

[35] Tim Salimans, Ian J. Goodfellow, Wojciech Zaremba, Vicki Cheung, Alec Radford, and Xi Chen. Improved techniques for training gans. In *Advances in Neural Information Processing Systems 29: Annual Conference on Neural Information Processing Systems 2016, December 5-10, 2016, Barcelona, Spain*, pages 2226–2234, 2016. 6

[36] Maurice Sion. On general minimax theorems. *Pacific J. Math.*, 8(1):171–176, 1958. 4

[37] Jianlin Su. Gan-qp: A novel gan framework without gradient vanishing and lipschitz constraint. 11 2018. 2, 5

[38] Sandeep Subramanian, Sai Rajeswar, Francis Dutil, Chris Pal, and Aaron C. Courville. Adversarial generation of natural language. In *Proceedings of the 2nd Workshop on Representation Learning for NLP, Rep4NLP@ACL 2017, Vancouver, Canada, August 3, 2017*, pages 241–251, 2017. 1

[39] Flood Sung, Yongxin Yang, Li Zhang, Tao Xiang, Philip H. S. Torr, and Timothy M. Hospedales. Learning to compare: Relation network for few-shot learning. In *2018 IEEE Conference on Computer Vision and Pattern Recognition, CVPR 2018, Salt Lake City, UT, USA, June 18-22, 2018*, pages 1199–1208, 2018. 3

[40] Christian Szegedy, Vincent Vanhoucke, Sergey Ioffe, Jonathon Shlens, and Zbigniew Wojna. Rethinking the inception architecture for computer vision. In *2016 IEEE Conference on Computer Vision and Pattern Recognition, CVPR 2016, Las Vegas, NV, USA, June 27-30, 2016*, pages 2818–2826, 2016. 6

[41] Hoang Thanh-Tung, Truyen Tran, and Svetha Venkatesh. Improving generalization and stability of generative adversarial networks. In *International Conference on Learning Representations*, 2019. 5

[42] Fisher Yu, Yinda Zhang, Shuran Song, Ari Seff, and Jianxiong Xiao. LSUN: construction of a large-scale image dataset using deep learning with humans in the loop. *CoRR*, abs/1506.03365, 2015. 2, 5

[43] Roman Zeyde, Michael Elad, and Matan Protter. On single image scale-up using sparse-representations. In *Curves and Surfaces - 7th International Conference, Avignon, France, June 24-30, 2010, Revised Selected Papers*, pages 711–730, 2010. 6

[44] Han Zhang, Ian J. Goodfellow, Dimitris N. Metaxas, and Augustus Odena. Self-attention generative adversarial networks. *CoRR*, abs/1805.08318, 2018. 1

[45] Han Zhang, Ian J. Goodfellow, Dimitris N. Metaxas, and Augustus Odena. Self-attention generative adversarial networks. *CoRR*, abs/1805.08318, 2018. 2